Supporting Information

Ottmann et al. 10.1073/pnas.0907587106

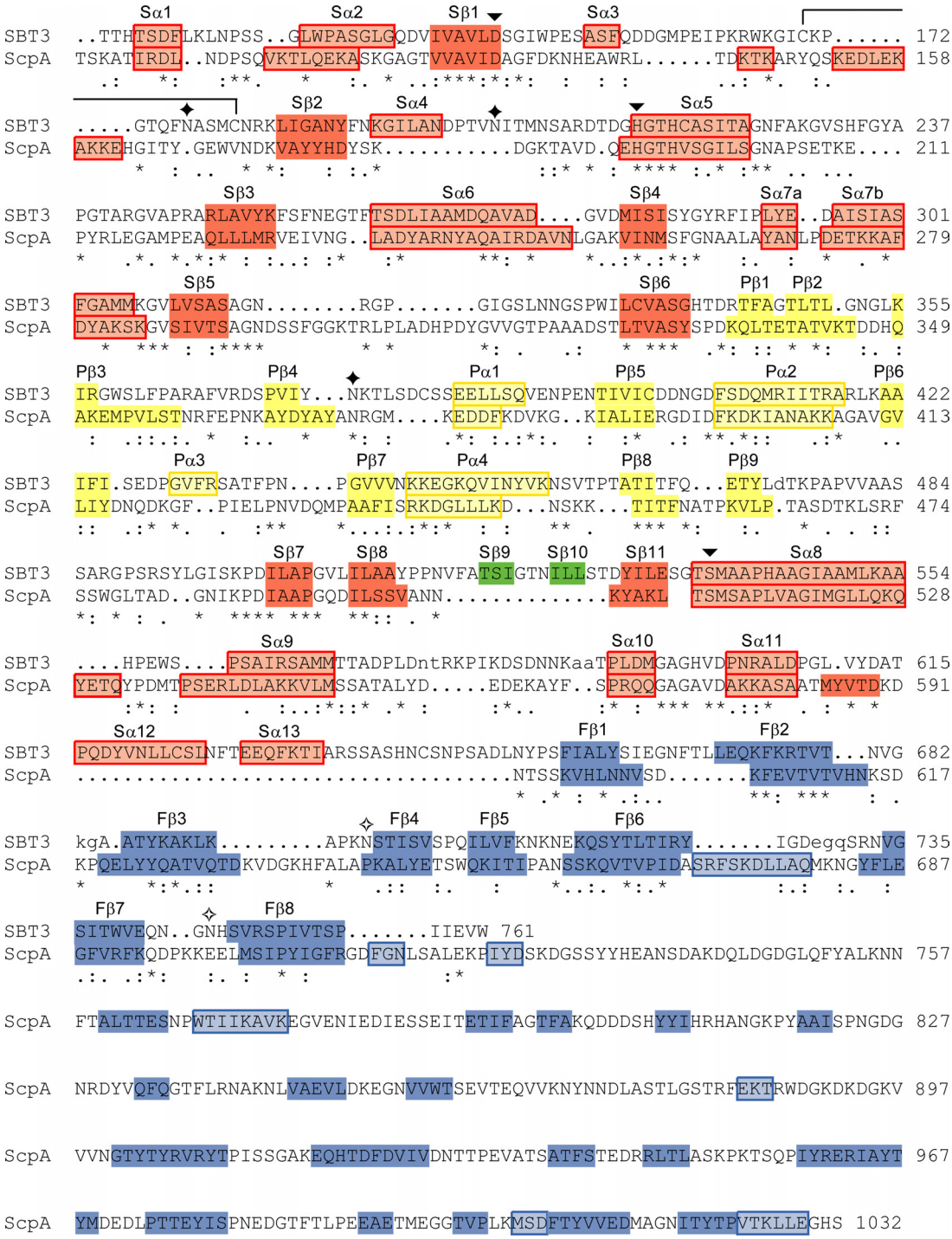

Fig. S1. Primary structure alignment of SBT3 with C5α peptidase from *Streptococcus pyogenes*. The Matchmaker tool in UCSF Chimera (http://www.cgl.ucsf.edu/chimera) was used to generate the alignment with 30% weighting of secondary structure score. Secondary structure elements are coloured in red, yellow and blue for the catalytic (S), PA (P), and fibronectin (F) domains, respectively. The additional β-hairpin in SBT3 is shown in green. Amino acid residues identical between SBT3 and C5α peptidase (ScpA) are indicated by an asterisk, conserved and semiconserved substitutions by colon and period, respectively. Active site residues are identified by solid triangles. Diamonds indicate N-linked glycosylation sites identified in the SBT3 structure (solid symbols) and by mass spectrometry (open symbols). The disulfide bridge between Cys-170 and Cys-181 is indicated. Lowercase letters were chosen to depict amino acid residues that were not visible in the electron density.

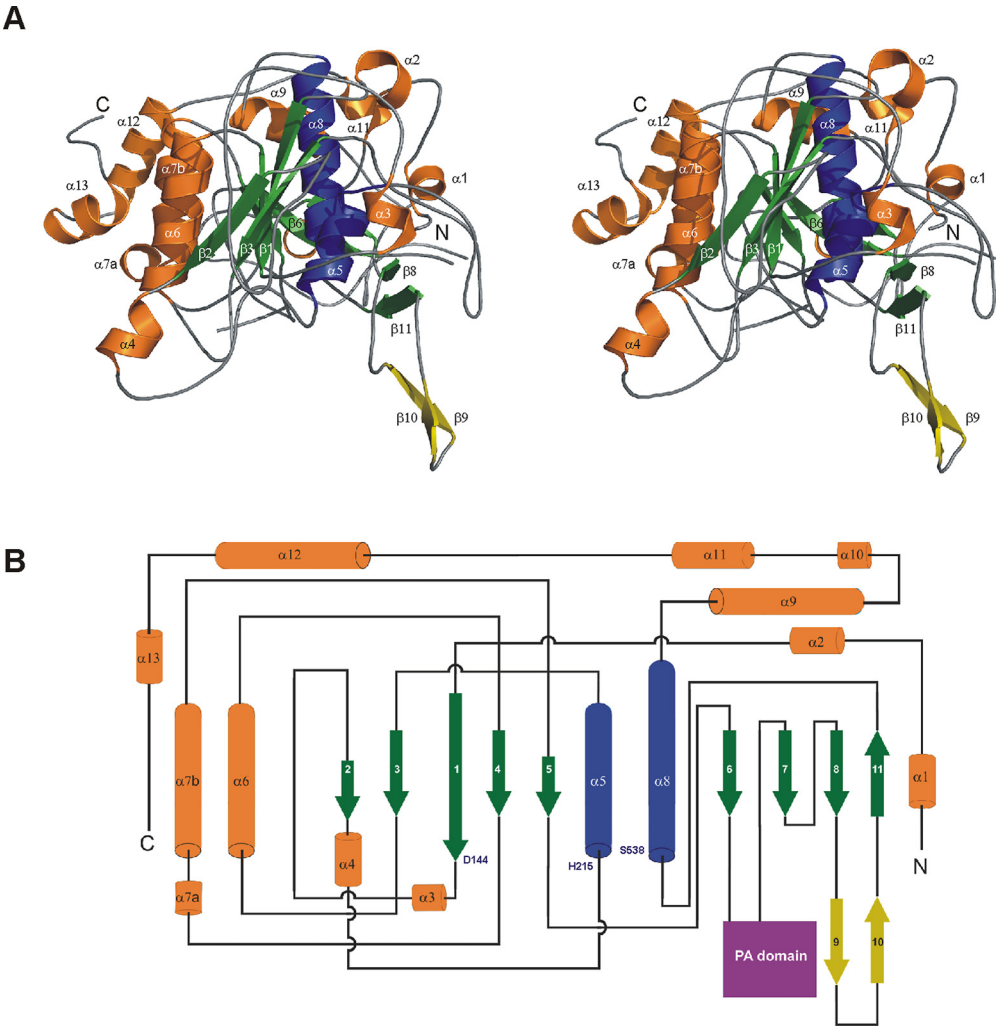

Fig. S2. Topology of the subtilisin domain of SBT3. (*A*) Stereoview of SBT3's subtilisin domain with central and peripheral helices colored in blue and orange, respectively, and core β-strands shown in green. The nonconserved β-hairpin is colored yellow. (*B*) Topology diagram of the subtilisin domain of SBT3. Color coding as in *A*. Positions of the catalytic triad residues are indicated by blue labels, the PA domain insertion is represented by a magenta rectangle.

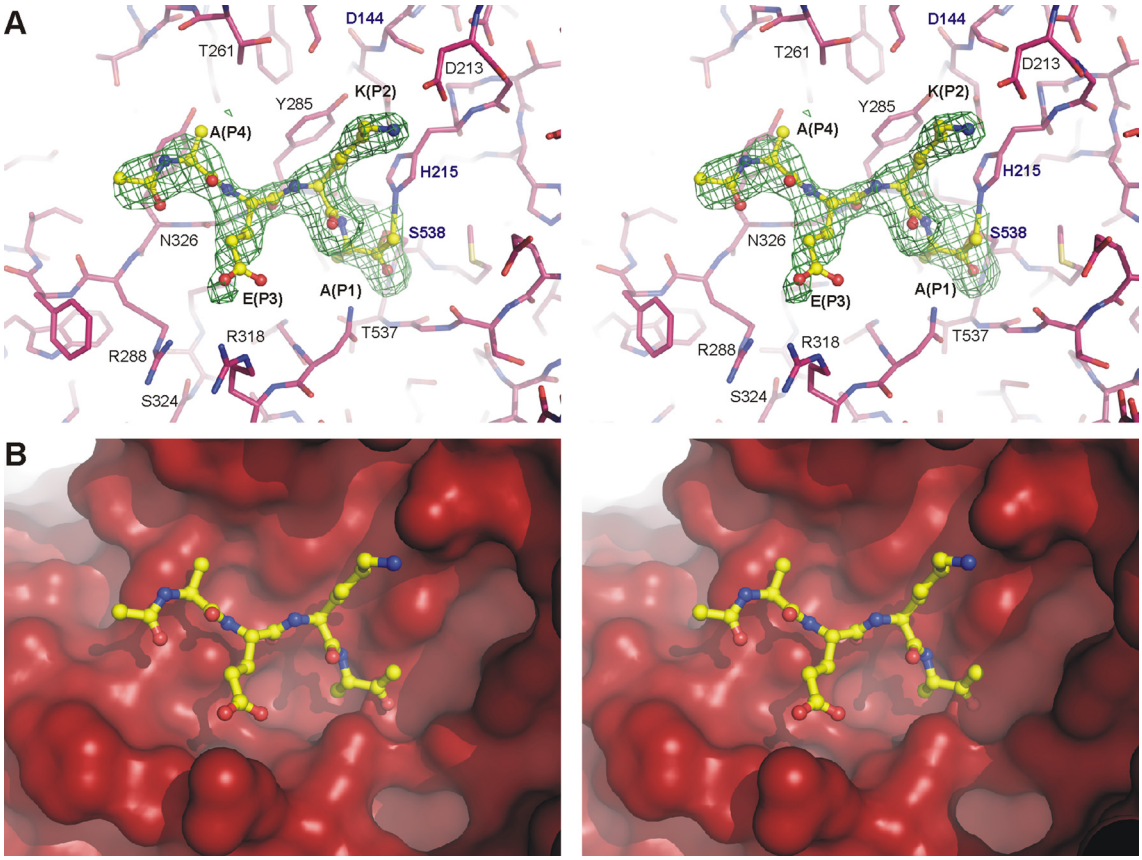

Fig. S3. Stereoview of the chloromethylketone inhibitor bound to the active site of SBT3. (*A*) Ball-and-stick model of Ac-Phe-Glu-Lys-Ala-CMK covalently bound to the active site of SBT3. Neighboring residues of SBT3 are displayed as magenta sticks, the Fo-Fc density map contoured at 2.5 σ is displayed as green mesh. (*B*) Solid surface representation of the active site cleft of SBT3 (red) bound with Ac- Phe -Glu-Lys-Ala-CMK.

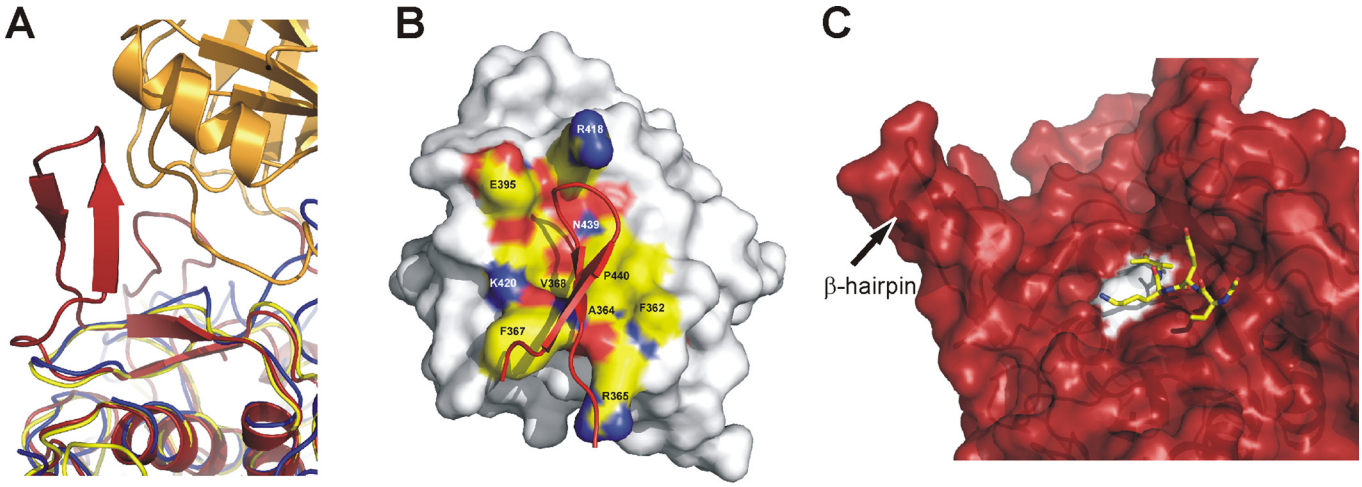

Fig. S4. The nonconserved β-hairpin insertion of SBT3's catalytic domain may play a role in dimerization-mediated activation. (*A*) Superimpositions of the subtilisin domain of SBT3 (red ribbon) with mouse furin (blue coil, PDB entry 1P8J) and the prokaryotic subtilisin BPN′ (yellow coil, PDB entry 1TM3). The PA domain of SBT3 is shown as orange ribbon. (*B*) Interaction surface of the PA-domain (solid surface) with the β-hairpin (red ribbon). Hydrophobic parts of the interface are coloured yellow, charged regions are coloured blue (positive) or red (negative). (*C*) Position of the β-hairpin relative to the active site of SBT3 (white, with bound CMK inhibitor displayed as yellow sticks).

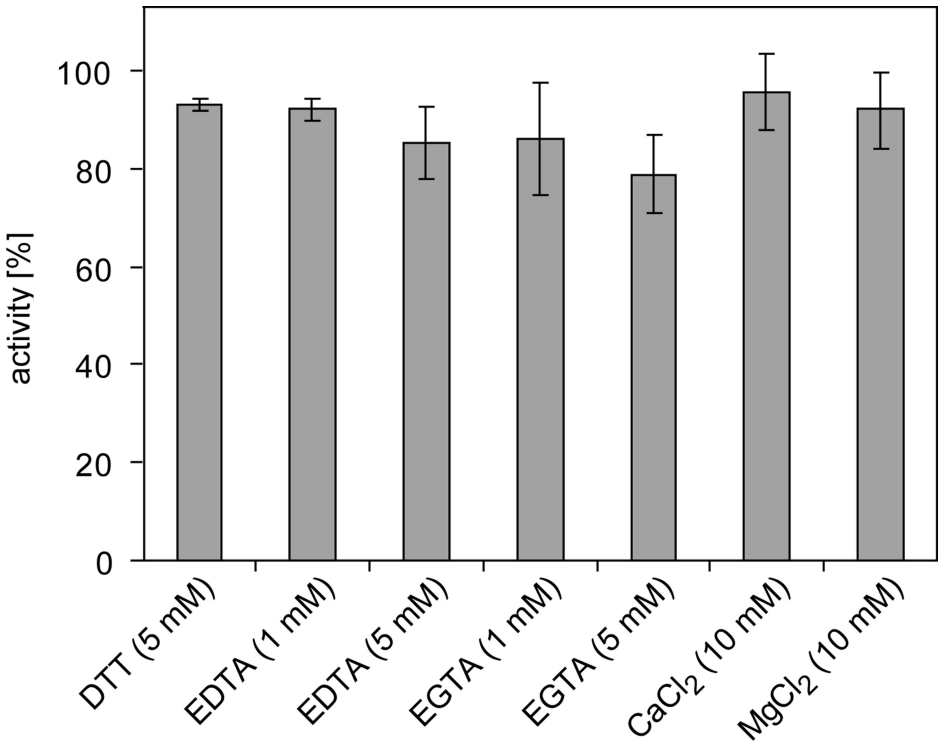

Fig. S5. SBT3 activity is not significantly different in presence or absence of calcium. SBT3 activity was assayed in presence of DTT (5 mM), EDTA (1 and 5 mM), EGTA (1 and 5 mM), $CaCl_2$ (10 mM), and $MgCl_2$ (10 mM) and is expressed in percentage of the control without additives. The data represent the mean +/− standard deviation of three independent experiments.

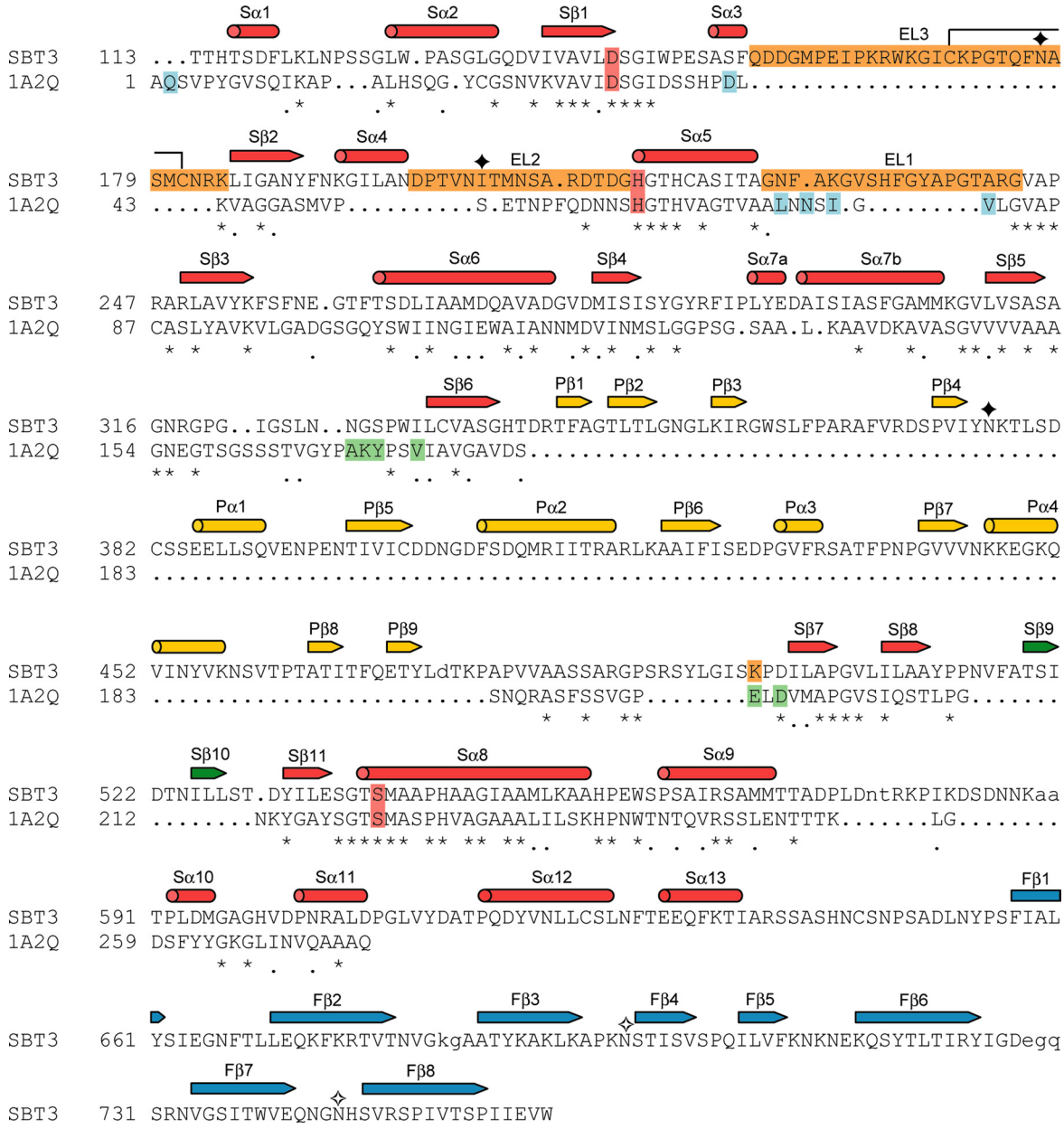

Fig. S6. Primary structure alignment of SBT3 with subtilisin BPN′ (1A2Q). The matchmaker tool in UCSF Chimera (http://www.cgl.ucsf.edu.chimera) was used to generate the alignment with 30% weighting of secondary structure score. Secondary structure elements of SBT3 are indicated in red, yellow, and blue for the catalytic (S), PA (P), and Fn III (F) domains, respectively. The additional β-hairpin is shown in green. Amino acid residues identical between SBT3 and BPN′ are indicated by an asterisk, conserved substitutions by dots. Active site residues are highlighted in red. BPN′ residues involved in calcium binding are indicated in blue (CA-1) and green (Ca-2), respectively. Extended loops (EL) 1–3 and Lys-498, which contribute to SBT3 stability in absence of calcium, are highlighted in orange. Diamonds indicate N-linked glycosylation sites identified in the SBT3 structure (solid symbols) and by mass spectrometry (open symbols). The disulfid bridge between Cys-170 and Cys-181 is indicated. Lowercase letters were chosen to depict amino acid residues that were not visible in the electron density.

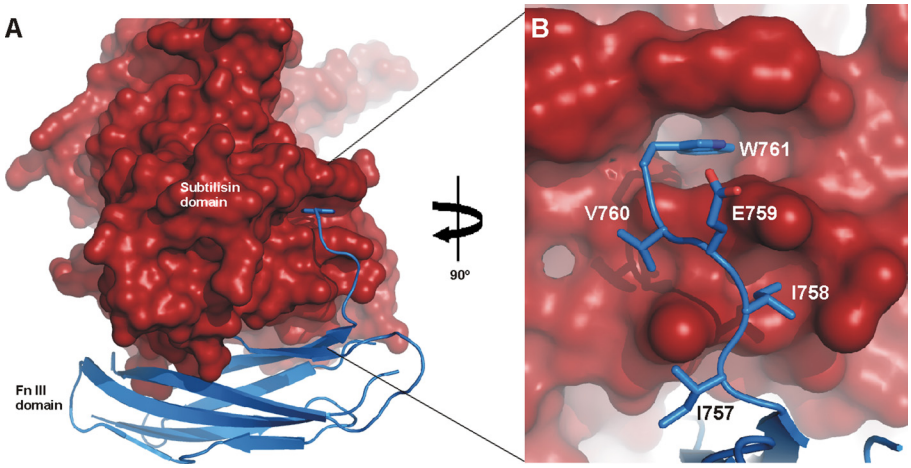

Fig. S7. Attachment of the FnIII domain (blue ribbons) to the subtilisin domain (red surface) in SBT3. (*A*) In addition to the main interface of these domains, the extreme C terminus of the FnIII domain constitutes a hydrophobic clamp that braces the FnIII domain to the subtilisin domain. (*B*) Detailed view of the five C-terminal amino acids of the FnIII domain binding to a hydrophobic patch of the subtilisin domain.

Table S1. Summary of crystallographic data

	Apo	FEKA
Data collection		
Space group	$P4_32_12$	$P4_32_12$
Cell dimensions		
a, Å	143.5	143.7
b, Å	143.5	143.7
c, Å	196.6	195.2
α, °	90.0	90.0
β, °	90.0	90.0
γ, °	90.0	90.0
Resolution, Å	25–2.5	20–2.6
R_{sym}	0.083 (0.327)*	0.081 (0.286)*
$I/\sigma I$	17.15 (4.32)	15.49 (5.41)
Completeness, %	99.5 (99.9)	99.5 (99.7)
Redundancy	7.7 (8.2)	6.5 (6.6)
Refinement		
Resolution, Å	2.5	2.6
No. reflections	67,526	59,937
R_{work}/R_{free}	0.2448/0.2798	0.2436/0.2898
No. atoms		
Protein	9,666	9,773
Water	547	527
B-factors		
Protein	49.28	39.74
Water	63.29	45.76
rmsd		
Bond lengths, Å	0.005	0.005
Bond angles, °	1.223	1.245

Crystallographic data are shown for native SBT3 (Apo) and the chloro-methyl-ketone-inhibited enzyme (FEKA).